Voicing classification of visual speech using convolutional neural networks

Thomas Le Cornu, Ben Milner

University of East Anglia
{t.le-cornu, b.milner}@uea.ac.uk

Abstract

The application of neural network and convolutional neural network (CNN) architectures is explored for the tasks of voicing classification (classifying frames as being either non-speech, unvoiced, or voiced) and voice activity detection (VAD) of visual speech. Experiments are conducted for both speaker dependent and speaker independent scenarios.

A Gaussian mixture model (GMM) baseline system is developed using standard image-based two-dimensional discrete cosine transform (2D-DCT) visual speech features, achieving speaker dependent accuracies of 79 % and 94 %, for voicing classification and VAD respectively. Additionally, a single-layer neural network system trained using the same visual features achieves accuracies of 86 % and 97 %. A novel technique using convolutional neural networks for visual speech feature extraction and classification is presented. The voicing classification and VAD results using the system are further improved to 88 % and 98 % respectively.

The speaker independent results show the neural network system to outperform both the GMM and CNN systems, achieving accuracies of 63 % for voicing classification, and 79 % for voice activity detection.

Index Terms: convolutional neural networks, voicing classification, visual speech

1. Introduction

The aim of this work is to explore using neural networks and convolutional neural networks for voicing classification and voice activity detection using visual speech features. Voicing classification is the challenge of classifying frames of speech (either audio, visual, or audiovisual) as being either non-speech, unvoiced, or voiced. The task of voice activity detection can be considered a more generalised version of the voicing classification task, classifying frames as speech or non-speech. By grouping the unvoiced and voiced classes together, the estimation of speech and non-speech results. The aim is to learn a function, f, to estimate the voicing class, $\hat{c}_t$, of the input visual speech feature vector, $\mathbf{v}_t$, described by,

$$\hat{c}_t = f(\mathbf{v}_t), \tag{1}$$

where $\hat{c}_t^{\mathrm{VC}} \in \{\text{ns, u, v}\}$ for voicing classification, and $\hat{c}_t^{\mathrm{VAD}} \in \{\text{ns, s}\}$ for voice activity detection.

Voice activity detection systems traditionally take audio speech as input. Problems occur as the signal-to-noise ratio is lowered due to increased background noise, with VAD accuracies decreasing as more non-speech frames become classified as speech frames [1]. For human speech perception, visual speech provides benefits by aiding with speaker localisation, providing additional segmental speech information, and providing extra place-of-articulation information that helps with the recognition of audibly confusable phonemes [2]. Including visual speech information to produce bimodal automatic speech recognition systems has proved beneficial especially when the channel conditions are less than satisfactory or significant amounts of audio noise are present [3].

A number of VAD systems have been developed that exploit the independence of the visual modality to background audio noise. In [4], visual speech features are extracted by applying principal component analysis to a matrix of pixel intensities localised about the mouth of the speaker. The most significant information is retained and then appended with first-order temporal derivatives, and modelled using two GMMs, one for non-speech and one for speech. Similarly, [5] uses GMMs to model visual speech information, using 2D-DCT visual speech features with the addition of first- and second-order temporal derivatives. Visual speech features obtained from active appearance models are commonly used for visual speech tasks such as lip reading, and are applied for voice activity detection in [6] with hidden Markov models (HMM) used to model the temporal information. The importance of temporal information is further highlighted in [7], where it was found that there is little lip-shape variation during periods of silence, and that the variations during speech periods is much greater. The use of optical flow visual speech features—describing the motion of pixels across contiguous frames—are used in [8] to directly incorporate temporal information into the visual VAD system.

This work extends previous systems by firstly, using a neural network for voicing classification and voice activity detection of input 2D-DCT visual speech features, and secondly, to explore the application of convolutional neural networks to the same tasks. The primary difference between the two systems is that the neural network takes visual speech features that have already been extracted from an image of the mouth of a speaker as input, whereas the CNN system processes the raw pixel intensities of the image and attempts to discover its own visual speech feature representation and then perform classification.

Recently, deep neural network (DNN) architectures (neural networks with greater than two hidden layers between the input and output layers) have been shown to outperform previous state-of-the-art GMM-HMM systems for automatic speech recognition [9]. The acoustic modelling capabilities are provided by the DNNs and the temporal variability is handled by the HMMs. A number of new DNN training techniques have further improved results [10]. Another neural network architecture, convolutional neural networks, have in recent years become the state-of-the-art for many computer vision tasks including large-scale image classification [11], and scene identification of videos [12]. Their application to audio speech features is applied in [13], showing improvements over DNN systems due to their ability to better model local correlations of the inputs, and translation variance of the acoustic speech existing due to speaker differences. Use of a different audio speech representation is investigated in [14], where input features take the form of spectrograms with information presented along the time and frequency axes.

The remainder of the paper is organised as follows. In Section 2 the use of neural networks for voicing classification is discussed, including how to reduce overfitting of training data and the architecture used. Convolutional neural networks are explored in Section 3 for both visual speech feature extraction and classification, including how to incorporate temporal information. The baseline GMM system is reviewed in Section 4. Data preprocessing and details of the speaker dependent and independent experiments is given in Section 5. Section 6 presents the voicing classification and voice activity detection results achieved for the baseline GMM, neural network, and CNN systems.

2. Neural network

Neural networks are learning algorithms where inputs are fed through a series of layers comprised of units (also called neurons), where each unit has a non-linear activation function. An example fully-connected neural network, where the units in layer m are connected to all of those in layer $m - 1$, is shown in Figure 1a. The hidden layers perform feature extraction by learning non-linear combinations of the inputs, where individually the features may not be particularly descriptive [15]. Care must be taken when training neural networks as they are prone to overfitting on the training set if there is a lack of training material. In this section, the use of neural networks is described for predicting voicing classification of input 2D-DCT visual speech features. Two neural network models are trained, `NN_DCT` for static visual features, and `NN_DCT_`Δ for visual features including temporal information.

2.1. Architecture

The network architecture used consists of a fully-connected network with a single hidden layer (consisting of 512 units) between the input layer and output softmax layer. A softmax function is commonly used in the output layer for multiclass classification problems to ensure the values from the final activation functions lie in the range 0 to 1, and that the sum of the values totals 1, giving a categorical probability distribution. Using greater numbers of hidden layers—producing deep neural networks—did not improve results enough to warrant the extra time required for training. The models are also relatively robust to the number of hidden units used, with values of 256, 512, and 1024, all producing comparable results.

Typical non-linear activation functions used in neural networks are the tanh and sigmoid functions, which both saturate given large input values. The Rectified Linear Unit (ReLU) is a non-saturating activation function proposed by [16], and is calculated as $f(x) = max(0, x)$. The benefit of building neural networks using ReLUs is that training concludes several times faster [11].

2.2. Dropout

Dropout [17] is a technique used in neural network architectures as a means to prevent overfitting of the training data. During training, neurons are selected at random and dropped. That is, the neuron and its connections are temporarily removed from the network for that particular instance or set of training examples.

Figure 1a shows an example fully-connected neural network with a single hidden layer. Figure 1b shows the same network after dropout has been applied. A probability of $p = 0.5$ is typically used for dropout applied to fully-connected hidden layers, and a probability closer to zero for dropping input units. The effect of applying dropout during training is to train a number of "thinned" models. For estimation, the classifications are then taken from the average of all the thinned-out networks. The effect is similar to training a large ensemble of models and averaging the predictions of each model [18].

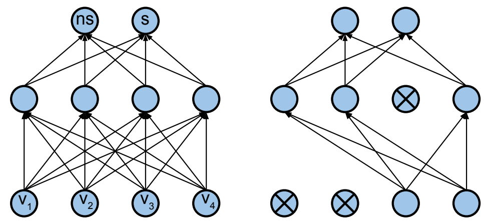

(a) Fully connected (b) Using dropout

Figure 1: A fully-connected network is shown in (a), and the same network after dropout has been applied in (b).

2.3. Training

The neural networks are trained using the resilient backpropagation algorithm [19]. L2 regularization is applied with a value of 0.001, and the learning rate is fixed at 0.001. The training visual vectors are grouped into mini-batches of 5000 examples, with z-score normalisation applied to the input 2D-DCT visual features. Training is completed once validation scores converge.

3. Convolutional neural networks

Convolutional neural networks have shown application for myriad computer-vision tasks such as handwritten digit recognition, and are motivated by the function of the primary visual cortex [15]. Convolutional layers differ from fully-connected layers (as shown in Figure 1a) in that the units in layer m are connected to only a local subset (representing a "receptive field") of the units in layer $m - 1$. Outputs from convolutional layers are called feature maps, and are calculated by convolving the inputs with multiple square matrices, which are analogous to filter kernels as used for image edge detectors or blurring. Weight sharing of the kernels ensures that they can extract features independent of where they occur in the input.

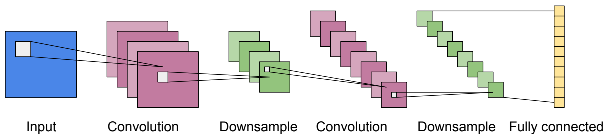

Figure 2: Example convolutional neural network architecture with two convolutional and downsampling layers, connected to a final fully-connected output layer.

An example CNN architecture is shown in Figure 2. An input image is convolved with four kernels producing four feature maps. A downsampling stage is performed following the convolution stage to reduce the size (width and height) of the feature maps. Max-pooling is used to perform this subsampling, whereby the maximum output of a small square window is taken. A further convolutional stage extracts eight feature maps, and is subsequently followed by another downsampling layer. The output of the final subsampled layer is then input to a fully-connected layer. Using deeper convolutional and fully-connected neural network architectures leads to the discovery of higher-level global features [20].

3.1. Architecture and training

The architecture used for this work follows Figure 2 and consists of two sets of convolutional–max-pooling–dropout layers, followed by a fully-connected hidden layer, and a final output softmax layer. The first convolutional layer consists of thirty-two filters of size 3×3, and the second, sixty-four filters of size 3×3. Non-overlapping max-pooling follows each convolutional layer with square regions of size 2×2. Dropout is then applied to each max-pooled layer with probability $p = 0.2$. The single fully-connected layer consists of 512 units, with dropout applied having probability $p = 0.5$. Rectified Linear Units are used throughout for activation functions.

Training is performed on an NVIDIA GRID K520 GPU card and takes approximately 5 h for the speaker dependent task and individual speaker independent runs. The visual frame pixel intensities are scaled to be in the range of zero to one, and training is performed using mini-batches of size 50. The network is trained using Nesterov's Accelerated Gradient Descent. Learning rate annealing is performed, decreasing the value by 1 % per epoch, and training is completed once validation scores converge.

3.2. Temporal information

Deep neural networks, used for large-vocabulary speech recognition, include temporal information through the simple concatenation of contiguous frames of audio features [9]. This approach cannot be used directly with convolutional neural networks at the input stage as the horizontal or vertical concatenation of frames would introduce issues at the boundaries of the images. An approach using early- and late-fusion for the inclusion of temporal information has shown success in large-scale video classification [12], and is applied here.

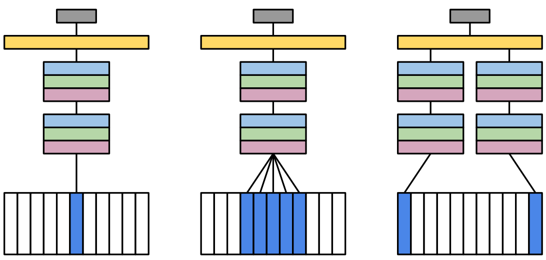

Figure 3: Static frame, and early- and late-fusion CNN architectures for including temporal information. Blue frames denote those that have current interest.

Figure 3 shows the single frame, early-fusion, and late-fusion architectures, including the convolutional and fully-connected connections as shown in Figure 2. Early-fusion functions at the first layer, extending the depth of the first convolutional layer filters to convolve across neighbouring video frames, for the detection of local motion direction. Late-fusion uses two separate convolutional columns for frames spaced a specific distance apart whose output is combined at the fully connected layers, therefore learning more global motion characteristics. However, the late-fusion technique is liable to miss the more fine-grained mouth movements important for the transitions between phones in the output audio speech. Experiments are conducted using a single frame system, `CNN_STATIC`, and a system using the early-fusion technique to stack three neighbouring frames together, called `CNN_STACK3`.

4. GMM baseline system

In [5], GMMs are used to model visual feature vectors for voice activity detection, and this forms the baseline to compare the neural network and CNN systems against. Vectors are grouped by class label and individual GMMs are trained—Φ^{s} for speech frames and Φ^{ns} for non-speech frames. Classification is performed by taking the $\arg\max$ of the probabilities produced by each class GMM, Φ^l, given the input visual vector, $\mathbf{v}_t$,

$$\hat{c}_t^{\text{VAD}} = \arg\max_l \left(p(\mathbf{v}_t | \Phi^l) \right), \tag{2}$$

where $l \in \{\text{ns}, \text{s}\}$. Applying the system to the task of voicing classification requires the training of three GMMs, one each for non-speech frames, unvoiced frames, and voiced frames, resulting in estimations given by,

$$\hat{c}_t^{\text{VC}} = \arg\max_l \left(p(\mathbf{v}_t | \Phi^l) \right), \tag{3}$$

where $l \in \{\text{ns}, \text{u}, \text{v}\}$. Through experimentation it was found that using sixteen clusters for each GMM gave the best performance. The two GMM models are named `GMM_DCT` and `GMM_DCT_`Δ, for the static and temporal models respectively.

5. Experiment description

Experiments are conducted on three systems for voicing classification and voice activity detection. A baseline GMM system (see Section 4), a neural network system (see Section 2), and a novel convolutional neural network system (see Section 3). For the speaker dependent scenarios, experiments are conducted for all three systems with static features and when temporal information has been added. For the speaker independent scenario, experiments are conducted on the GMM and neural network systems using first-order temporal derivatives, and on both CNN systems.

5.1. Dataset

The GRID audiovisual dataset [21] is used for the experiments. The dataset includes video of thirty-four speakers each having produced 1000 utterances. The videos are three seconds in length with twenty-five frames per second, giving seventy-five frames per video. The resolution of each frame is 576×720 pixels, and contains RGB channel information. Word time-alignment files are included for each utterances that describes the start and end points for each word of the utterance, as well as periods of silence.

The speaker dependent task uses all visual data, totalling approximately 50 minutes, for the speaker (speaker 6 in the corpus), and is split with 80 % for training and 20 % for testing. Data from nine speakers is used for the speaker independent task. One hundred utterances are selected from each of the nine speakers (speakers 1–7, 10, and 12), therefore ensuring the training/testing data split is roughly equal for both the speaker dependent and independent tasks. k-fold cross validation is used for the speaker independent experiments, segmenting the training data into that from eight of the speakers, and then performing testing on the held-out speaker. This is repeated for all permutations, and the final accuracy results are averaged.

5.2. Visual preprocessing

The video data is up-sampled to 100 Hz to match a typical audio speech frame rate of 10 ms. The FFMPEG suite of multimedia tools [22] is used to extract greyscale visual frames at the required rate. Images of size 96×96 pixels are extracted about a centre-point of the mouth calculated from landmark data, and resized to 64×64 pixels. Figure 5a shows an example extracted mouth image.

Image-based visual speech features derived from a two-dimensional discrete cosine transform are used for the neural network and GMM systems. Features are extracted from a matrix of pixel intensities that is centred on a tracked mouth centre point. A 2D-DCT is applied to produce a coefficient matrix from which a J-dimensional visual vector is obtained by extracting coefficients in a zigzag order from the lower coefficient region of the matrix [23]. The first coefficient (the DC term) is discarded and 35 coefficients are retained.

5.3. Voicing classification labels

To measure voicing classification and voice activity detection accuracy, reference labels are required. Processing of the word time-alignment files is performed to provide VAD data, that is, the non-speech and speech classes.

$$c_t^{\mathrm{VAD}} = \begin{cases} \mathrm{s} & \text{if } x(t) \text{ is speech} \\ \mathrm{ns} & \text{otherwise} \end{cases} \tag{4}$$

For the voicing classification task, labels are required for each frame of speech, t, classifying each as either non-speech, unvoiced, or voiced. The PEFAC pitch-extraction algorithm [24] is used to provide a probability that a given frame of speech is voiced. The voiced speech probabilities output from PEFAC are thresholded, with frames of speech having probability $p(t) \geq 0.5$ labelled as voiced. Frames classified as speech using the voice activity data, described by Equation 4, that are not classified as voiced using PEFAC, are labelled as unvoiced.

$$c_t^{\mathrm{VC}} = \begin{cases} \mathrm{v} & \text{if } p(t) \geq 0.5 \\ \mathrm{u} & \text{if speech and } p(t) < 0.5 \\ \mathrm{ns} & \text{otherwise} \end{cases} \tag{5}$$

Equation 5 describes the class labels assigned to each frame. Median filtering is performed on the thresholded probabilities to remove isolated values.

6. Evaluation

In this section, accuracy results are presented for voicing classification and voice activity detection of the three systems for the speaker dependent and speaker independent scenarios. Accuracies are recorded for the multiclass voicing classification task, and then by grouping the unvoiced and voiced estimations, the VAD results are obtained. Lastly, intuition is given for the filter kernels learnt by the CNN systems and the convolutions they produce.

6.1. Speaker dependent results

Table 1 shows voicing classification and voice activity detection accuracies for the speaker dependent task. The CNN_STACK3 achieves the best accuracy for voicing classification, with a score of 87.55 %. Accordingly, the same system outperforms both the GMM and neural network systems for voice activity detection with an accuracy of 97.66 %. Surprisingly, the CNN_STATIC system is able to achieve 86.05 % voicing accuracy using static information. In comparison, the static GMM and neural network systems achieve accuracies of 11.76 % and 6.44 % lower respectively. This suggests that by using convolutional neural networks, suitably descriptive visual speech feature representations can be found.

Table 1: Speaker dependent VAD and voicing classification accuracies in per cent.

Configuration	Voicing accuracy	VAD accuracy
GMM_DCT	74.29	92.61
GMM_DCT_Δ	78.99	94.34
NN_DCT	79.61	96.00
NN_DCT_Δ	86.35	96.80
CNN_STATIC	86.05	96.99
CNN_STACK3	**87.55**	**97.66**

Increased voicing classification accuracy by including temporal information is readily apparent for both the neural network and GMM systems. A classification accuracy increase of 4.7 % and 6.7 % is gained for the GMM and neural network respectively. However, the same increase does not occur when using the CNN. Interestingly, it appears that due to the only slight increase in performance between the CNN_STATIC and CNN_STACK3 systems of 1.5 %, using the early-fusion technique for including temporal information in the CNN architecture is not ideal for this work, and that other techniques for temporal fusion could result in a greater accuracy.

Table 2: Confusion matrix of per cent classification accuracy using the CNN_STACK3 speaker dependent model.

	Non-speech	Unvoiced	Voiced
Non-speech	98.23	1.49	0.28
Unvoiced	5.91	66.84	27.25
Voiced	0.72	8.93	90.36

Table 2 shows a confusion matrix for classification accuracies for the speaker dependent CNN_STACK3 model. The majority of voicing classification errors occur with the misclassification of unvoiced frames as voiced frames, with 27.25 % doing so. The problem experienced with voicing classification occurs when different voiced and unvoiced phonemes have the same visual speech realisations. Phonemes sharing the same visual realisations can be grouped by phoneme equivalence class (PEC), a generalisation of the viseme for the grouping of visually similar phonemes proposed by [25]. Regarding problems of voicing classification, a PEC comprised of /s t z/ consists of two unvoiced consonants, /s/ and /t/, and a voiced consonant, /z/, for example. A PEC comprised of /f v/ has a voiced and unvoiced consonant. The PECs described are taken from [26]. Voice activity detection errors can be seen where unvoiced or voiced frames are classified as non-speech, and vice versa. The problem in this case is that visual realisations of certain PECs have a mouth shape that is very visually similar to the neutral. For example, this is the case with the PEC comprised of the phonemes /b m p/. The majority of errors occur when unvoiced frames are misclassified as non-speech frames, happening for

5.91 % of unvoiced frames.

6.2. Speaker independent results

The speaker independent results are displayed in Table 3. The NN_DCT_Δ system achieves accuracies of 63.13 % and 78.69 % for voicing classification and voice activity detection respectively, outperforming the GMM_DCT_Δ system by 11.02 % and 8.19 % for each task. The speaker independent results are considerably worse than the speaker dependent results, suggesting that greater attention needs to be spent on removing visual speech feature differences existing between speakers.

Table 3: Speaker independent VAD and voicing classification accuracies in per cent.

Configuration	Voicing accuracy	VAD accuracy
GMM_DCT_Δ	52.11	70.50
NN_DCT_Δ	**63.13**	**78.69**
CNN_STATIC	59.02	74.07
CNN_STACK3	59.02	74.68

The CNN systems do not perform as well for the speaker independent scenario. The best system, CNN_STACK3, using temporal information, achieves accuracies of 59.02 % and 74.68 % for voicing classification and VAD. There is also not a noticeable difference between the static and temporal models, which again suggests that other methods of including temporal information in the convolutional neural network architecture would increase results.

Table 4: Confusion matrix of classification accuracies in per cent for speaker one using the CNN_STACK3 speaker independent model.

	Non-speech	Unvoiced	Voiced
Non-speech	90.58	8.94	0.47
Unvoiced	34.70	54.80	10.50
Voiced	14.58	43.98	41.44

Table 4 shows a confusion matrix for classification accuracies for speaker one trained on the other eight speakers using the CNN_STACK3 system. In comparison to Table 2, it can be seen that the majority of voicing classification errors come from an increase in voiced frames being misclassified as unvoiced, and from unvoiced frames being misclassified as non-speech. In terms of voice activity detection, there is a large increase in the number of unvoiced and voiced frames that are misclassified as non-speech.

6.3. Visualisation of learnt filters and convolutions

Visualisations of the thirty-two 3×3 filter kernels learnt by the first convolutional layer are shown in Figure 4. The kernel values have been resized (using cubic interpolation) and normalised in the range of zero to one for display. A variety of the learnt kernels show edge detection properties. For example, kernels 17 and 32 highlight horizontal edges, whereas kernels 22 and 25 highlight diagonal edges.

As shown in Figure 2, the result of convolving an input image with the filter kernels is to produce a number of feature maps. Figure 5a shows an original mouth image as would be input to the CNN, and a selection of feature maps after convolution with the kernels. Convolutions with kernels 2 and 32 (see Figures 5b and 5d) serve to highlight the area of the inner mouth, effectively removing information of the skin and lips, with kernel 2 exhibiting more blurring than kernel 32. The image convolved with kernel 25 (see Figure 5c) shows how the diagonal edges have been highlighted, as can be seen by the greater pixel intensity on the upper-left edges of the teeth, and in the lower-right corner of the inner mouth.

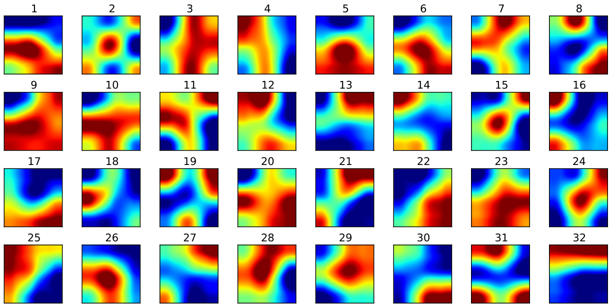

Figure 4: Thirty-two kernels learnt in the first convolutional layer for the speaker dependent task. Blue values are lower, red are higher.

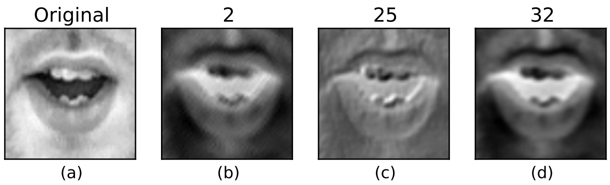

Figure 5: Example original mouth image, and when convolved with filter kernels 2, 25, and 32, as depicted in Figure 4.

7. Conclusion

For the speaker dependent scenario the novel convolutional neural network approach outperforms the baseline GMM and neural network systems for both voicing classification and voice activity detection. The high accuracy achieved for the CNN using static information shows promise for their ability to discover descriptive visual speech feature representations. As such, their use in current audiovisual VADs for the visual stream should prove beneficial. Similarly, their use in other applications, such as lip reading and audiovisual automatic speech recognition, could improve accuracy for speaker dependent scenarios. A further increase in accuracy for voicing classification could be attained by better incorporating temporal information into the system.

The neural network outperforms both the GMM and CNN systems for the speaker independent scenario, presumably as the hidden layer feature extraction can better ignore the between-speaker differences. Further work on removing the differences between visual speech features of different speakers would, therefore, likely increase the speaker independent results achieved. Regarding the convolutional neural networks, exploring different architectures in depth, the application of state-of-the-art techniques, and a large increase in the amount of speaker training data used, should all serve to increase accuracy.

8. References

[1] J. Ramırez, J. C. Segura, C. Benıtez, A. De La Torre, and A. Rubio, "Efficient voice activity detection algorithms using long-term speech information," *Speech communication*, vol. 42, no. 3, pp. 271–287, 2004.

[2] Q. Summerfield, "Some preliminaries to a comprehensive account of audio-visual speech perception," in *Hearing by Eye: The Psychology of Lip-Reading*, B. Dodd and R. Campbell, Eds. Lawrence Erlbaum Associates, 1987.

[3] S. Dupont and J. Luettin, "Audio-visual speech modeling for continuous speech recognition," *Multimedia, IEEE Transactions on*, vol. 2, no. 3, pp. 141–151, 2000.

[4] P. Liu and Z. Wang, "Voice activity detection using visual information," in *Acoustics, Speech, and Signal Processing, 2004. Proceedings.(ICASSP'04). IEEE International Conference on*, vol. 1. IEEE, 2004, pp. I–609.

[5] I. Almajai and B. Milner, "Using audio-visual features for robust voice activity detection in clean and noisy speech," in *Proc. EUSIPCO*, vol. 86, 2008.

[6] A. Aubrey, B. Rivet, Y. Hicks, L. Girin, J. Chambers, and C. Jutten, "Two novel visual voice activity detectors based on appearance models and retinal filltering," in *15th European Signal Processing Conference (EUSIPCO-2007)*, 2007.

[7] D. Sodoyer, B. Rivet, L. Girin, J.-L. Schwartz, and C. Jutten, "An analysis of visual speech information applied to voice activity detection," in *Acoustics, Speech and Signal Processing, 2006. ICASSP 2006 Proceedings. 2006 IEEE International Conference on*, vol. 1. IEEE, 2006, pp. I–I.

[8] A. Aubrey, Y. Hicks, and J. Chambers, "Visual voice activity detection with optical flow," *IET image processing*, vol. 4, no. 6, pp. 463–472, 2010.

[9] G. Hinton, L. Deng, D. Yu, G. E. Dahl, A.-r. Mohamed, N. Jaitly, A. Senior, V. Vanhoucke, P. Nguyen, T. N. Sainath *et al.*, "Deep neural networks for acoustic modeling in speech recognition: The shared views of four research groups," *Signal Processing Magazine, IEEE*, vol. 29, no. 6, pp. 82–97, 2012.

[10] G. E. Dahl, T. N. Sainath, and G. E. Hinton, "Improving deep neural networks for LVCSR using rectified linear units and dropout," in *Acoustics, Speech and Signal Processing (ICASSP), 2013 IEEE International Conference on*. IEEE, 2013, pp. 8609–8613.

[11] A. Krizhevsky, I. Sutskever, and G. E. Hinton, "ImageNet classification with deep convolutional neural networks," in *Advances in neural information processing systems*, 2012, pp. 1097–1105.

[12] A. Karpathy, G. Toderici, S. Shetty, T. Leung, R. Sukthankar, and L. Fei-Fei, "Large-scale video classification with convolutional neural networks," in *Computer Vision and Pattern Recognition (CVPR), 2014 IEEE Conference on*. IEEE, 2014, pp. 1725–1732.

[13] T. N. Sainath, A.-r. Mohamed, B. Kingsbury, and B. Ramabhadran, "Deep convolutional neural networks for LVCSR," in *Acoustics, Speech and Signal Processing (ICASSP), 2013 IEEE International Conference on*. IEEE, 2013, pp. 8614–8618.

[14] O. Abdel-Hamid, L. Deng, and D. Yu, "Exploring convolutional neural network structures and optimization techniques for speech recognition." in *INTERSPEECH*, 2013, pp. 3366–3370.

[15] K. P. Murphy, *Machine learning: a probabilistic perspective*. MIT press, 2012.

[16] V. Nair and G. E. Hinton, "Rectified linear units improve restricted boltzmann machines," in *Proceedings of the 27th International Conference on Machine Learning (ICML-10)*, 2010, pp. 807–814.

[17] N. Srivastava, G. Hinton, A. Krizhevsky, I. Sutskever, and R. Salakhutdinov, "Dropout: A simple way to prevent neural networks from overfitting," *The Journal of Machine Learning Research*, vol. 15, no. 1, pp. 1929–1958, 2014.

[18] I. J. Goodfellow, D. Warde-Farley, M. Mirza, A. Courville, and Y. Bengio, "Maxout networks," *arXiv preprint arXiv:1302.4389*, 2013.

[19] M. Riedmiller and H. Braun, "A direct adaptive method for faster backpropagation learning: The RPROP algorithm," in *Neural Networks, 1993., IEEE International Conference on*. IEEE, 1993, pp. 586–591.

[20] Y. Sun, X. Wang, and X. Tang, "Deep convolutional network cascade for facial point detection," in *Computer Vision and Pattern Recognition (CVPR), 2013 IEEE Conference on*. IEEE, 2013, pp. 3476–3483.

[21] M. Cooke, J. Barker, S. Cunningham, and X. Shao, "An audio-visual corpus for speech perception and automatic speech recognition," *The Journal of the Acoustical Society of America*, vol. 120, no. 5, pp. 2421–2424, 2006.

[22] "FFmpeg," https://www.ffmpeg.org/, accessed: 28/04/2015.

[23] K. Sayood, *Introduction to data compression*. Morgan-Kaufmann, 2000.

[24] S. Gonzalez and M. Brookes, "PEFAC-a pitch estimation algorithm robust to high levels of noise," *Audio, Speech, and Language Processing, IEEE/ACM Transactions on*, vol. 22, no. 2, pp. 518–530, 2014.

[25] E. T. Auer Jr and L. E. Bernstein, "Speechreading and the structure of the lexicon: Computationally modeling the effects of reduced phonetic distinctiveness on lexical uniqueness," *The Journal of the Acoustical Society of America*, vol. 102, no. 6, pp. 3704–3710, 1997.

[26] L. Bernstein, "Visual speech perception," *AudioVisual Speech Processing*, pp. 21–39, 2012.